

Growth and characterization of $Zn_xSn_{1-x}Se$ films for use in thin film solar cells

T.M. Razykov^{a,*}, A. Bosio^b, B. Ergashev^a, K.M. Kouchkarov^a, A. Romeo^c, N. Romeo^b,
R. Yuldoshov^a, M. Baiev^a, M. Makhmudov^a, J. Bekmirzoyev^a, R. Khurramov^a, E. Fazylov^a

^a Physical-Technical Institute, Uzbek Academy of Sciences, Chingiz Aytmatov Street 2B, Tashkent 700084, Uzbekistan

^b University of Parma, G.P. Usberti 7/A, 43124 Parma, Italy

^c Universita' di Verona, Ca' Vignale 2- Strada Le Grazie 15, 37134 Verona, Italy

ARTICLE INFO

Keywords:

$Zn_xSn_{1-x}Se$ films
X-ray
Morphology
Grain size
Conductivity

ABSTRACT

We have fabricated $Zn_xSn_{1-x}Se$ (ZTSe) films for the first time. Samples were fabricated by chemical molecular beam deposition method at atmospheric pressure in hydrogen flow. ZnSe and SnSe powders with 99.999% purity were used as precursors. The temperature of precursors varied in the range of (850–950) °C. Films were deposited at substrate temperature of (500–600) °C. Borosilicate glass was used as a substrate. We have studied ZTSe films by EDS, XRD and SEM. The samples had orthorhombic and cubic structures depending on composition. Results of EDS have shown that stoichiometric composition of samples moved to ZnSe side by increasing with substrate temperature. SEM pictures have shown that samples had polycrystalline structure. The grain size varied in the range of (2–15) μm . The grain size of samples increased from (2–5) μm to (15–20) μm for substrate temperatures of 500 °C and 550 °C respectively. While, at a substrate temperature of 600 °C the grain size decreased up to (3–5) μm , possibly, because of increasing of ZnSe content. XRD analysis has shown that samples have ZnSe, SnSe, Se and Sn phases. The band gap of samples varied in the range of 1.0–2.0 eV depending on the film compositions. An inversion of the conductivity type was found: samples fabricated at 500 °C and 550 °C performed of p-type conductivity; while samples fabricated at 600 °C showed n-type conductivity.

1. Introduction

Generating electricity from solar photovoltaic (PV) power systems is continuously growing around the world. It is estimated that more than 1.8% of the annual global electricity demand in 2017 was covered by solar photovoltaic power systems. In terms of amount of energy, this is about 500,000 GWh in one year. This figure represent a huge development of the past years, much faster than all predictions made. Solar PV has also gained cost-competitiveness. Compared with all other renewable sources, the solar PV electricity is one of the least-cost option. These days the PV electricity is as low as below 5–7 USD cents/kWh. Europe has been the most important driver of the global solar PV market over the past ten years. After Europe, the USA, Asia, China, and Japan have seen further market growth representing the largest markets in 2018.

Currently, crystalline and multi-crystalline wafer silicon cover 85% of the photovoltaic market. However, producing power with these cells remains expensive compared to conventional power generation. Average spot polysilicon price has crossed below the \$8/kg threshold

for the first time, according to PV Insights (<https://www.pv-magazine.com/2019/08/20/polysilicon-prices-to-rebound-in-september/>). In order to reduce production costs, thin film solar cells have been developed, in particular cadmium telluride and on copper indium gallium diselenide based solar cells. The highest efficiency values reported for CdTe and Cu(In, Ga)Se₂ based solar cells are 22.1% (http://www.pv-magazine.com/news/details/beitrag/first-solar-sets-new-cadmium-telluride-thin-film-cell-efficiency-record-at-22.1_100023341/#ixzz415kiS7YW) and 23.2% (<http://www.renewableenergyworld.com/rea/blog/post/2014/03/two-thin-film-solar-efficiency-records-broken-this-week?cmpid=WNL-Wednesday-March5-2014>) in laboratory conditions and 16.1% (<http://www.businesswire.com/news/home/20130409006059/en/Solar-Sets-CdTe-Module-Efficiency-World-Record>) and 17% (Green et al., 2013) for modules, respectively. Despite these achievements, problems still remain: in the former cells, there is a particular need to control disposal after use due to the presence of cadmium; in the latter cells, the scarcity of indium supply and the high material cost of indium and gallium impelled researchers to look for alternative photovoltaic materials.

* Corresponding author.

E-mail address: razykov@uzsci.net (T.M. Razykov).

<https://doi.org/10.1016/j.solener.2019.09.072>

Received 30 July 2019; Received in revised form 18 September 2019; Accepted 21 September 2019

0038-092X/ © 2019 International Solar Energy Society. Published by Elsevier Ltd. All rights reserved.

Therefore, many research centers and laboratories conduct research to replace the abovementioned expensive materials with Earth abundant elements based compounds (Le Donne et al., 2019) such as $\text{Cu}_2\text{ZnSnS}_4$ (CZTS). This absorber layer is not only cost effective and non-toxic, but also has similar optical properties to that of $\text{Cu}(\text{In}, \text{Ga})\text{Se}_2$ absorber layer. CZTS based solar cells has achieved the efficiency of 12.6% (Wang et al., 2014) reported by the IBM research center. However, this efficiency is still lower than that of $\text{Cu}(\text{In}, \text{Ga})\text{Se}_2$. According to Todarov et al. (2013), low efficiency of CZTS is due to the complexity of sample preparation methods and controlling the film composition.

Novel low cost and high efficiency zinc and tin selenide ($\text{Zn}_x\text{Sn}_{1-x}\text{Se}$) thin film solar cells are without these drawbacks. However, there is no information in the literature regarding this new material. This compound has excellent photovoltaic properties:

- (i) the band gap can be varied in a very wide range of (0.9–2.7) eV, which is suitable for single junction thin film solar cells with optimum direct energy band gap of 1.45 eV (efficiency in the range of (20–25)%) and double junction cells in which the absorber layers could have, with band gaps of $E_{g1} = 1.0$ eV and $E_{g2} = 1.7$ eV, efficiencies of (20–25)% and (30–35)% respectively,
- (ii) absorption coefficient is 10^4 – 10^5 cm^{-1} , which means that an absorber thickness of (0.5–1.0) μm is enough to fabricate high efficiency cells,
- (iii) it consists of abundant, non-toxic and low-cost elements and it can be made either *n*-type or *p*-type conductivity.

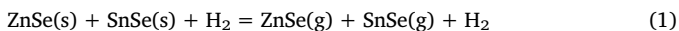
Earlier, we had discussed characteristics of SnSe films in (Razykov et al., 2018). In this paper morphology, structure, optical band gap and conductivity of $\text{Zn}_x\text{Sn}_{1-x}\text{Se}$ (ZTSe) films with different compositions are discussed.

2. Experiment

Samples were fabricated by chemical molecular beam deposition method at atmospheric pressure in hydrogen flow (Razykov, 1991). ZnSe and SnSe powders with 99.999% purity were used as precursors. The temperature of precursors varied in the range of (850–950) °C. Films were deposited at substrate temperatures of (500–600) °C. Borosilicate glass was used as a substrate. We have studied ZTSe films by energy dispersive X-ray spectrometry (EDS), X-ray diffraction (XRD), scanning electron microscopy (SEM) and four probe method. The crystal structure of films were investigated by XRD measurements using a “Panalytical Empyrean” diffractometer (Cu $K\alpha$ radiation, $\lambda = 1.5418$ Å) with a wide-angle measurements of 2θ in the range of (10–90)° with a measurement steps of 0.01°. The experimental results were studied using the ‘Joint Committee on Powder Diffraction Standard’ (JCPDS, № 15-0861 for SnSe films). Morphological and chemical composition of the samples was investigated using a SEM-EVO MA 10 and an EDX (Oxford Instrument - Aztec Energy Advanced X-act SDD) at an electron acceleration voltage of 15 kV, respectively. To perform electrical measurements, ohmic contacts were realized by vacuum deposition of silver on the film surfaces. The conductivity of films was measured by van der Pau method. The type of conductivity of the samples was determined by thermoelectric effect. The thickness of the films was determined using micro-interferometer MII-4.

3. Results and discussion

At the evaporation temperature ZnSe and SnSe powders transfer into the vapor phase:



Then $\text{ZnSe}(g)$ and $\text{SnSe}(g)$ dissociate into $\text{Zn}(g)$, $\text{Sn}(g)$ and $\text{Se}_2(g)$:

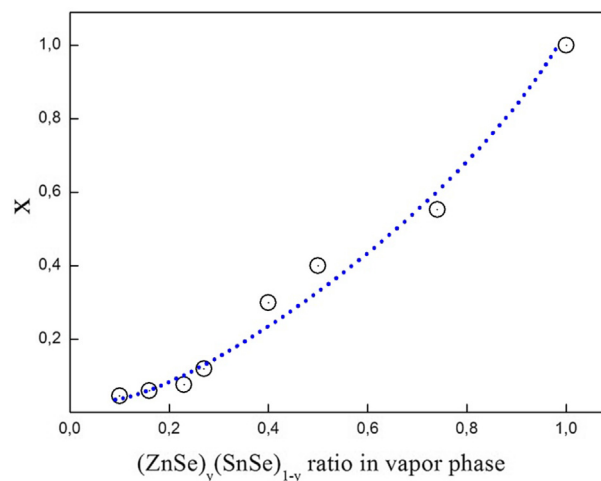
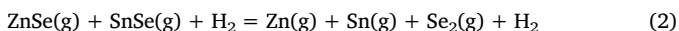
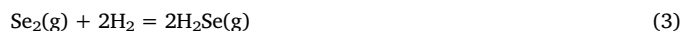
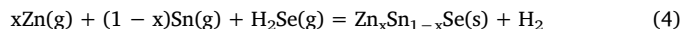


Fig. 1. The dependence of films composition on the vapor phase mixture (evaporated amount) of the $(\text{ZnSe})/(\text{SnSe})$ ratio. (The substrate temperature is 550 °C).

$\text{Se}_2(g)$ reacts with hydrogen and hydrogen selenide is formed:



Zn and Sn atoms and H_2Se molecules reach the surface of the substrate and ZTSe films is formed as a result of their interaction:



We controlled ZTSe films composition by changing the vapor phase mixture (evaporated amount) of $(\text{ZnSe})/(\text{SnSe})$ ratio. The dependence of the film compositions on the vapor phase mixture is shown in Fig. 1. It is seen that this dependence has almost a quadratic behavior. It was observed that the composition of $\text{Zn}_x\text{Sn}_{1-x}\text{Se}$ films strongly depends on the substrate temperature. As seen from Fig. 2, the composition of $\text{Zn}_x\text{Sn}_{1-x}\text{Se}$ films moves to ZnSe side with the substrate temperature. This shows that the sublimation of Zn atoms increases with the substrate temperature. It might be due to the high vapor pressure of Zn in comparison with Sn at the deposition temperatures. While Sn vapors being carried away from the deposition zone by hydrogen. Content of Sn in ZTSe increases with decreasing the substrate temperature.

X-ray diffraction patterns of ZTSe films with different compositions are shown in Fig. 3. The spectra were obtained by scanning 2θ in the range 20–60°, with a grazing angle equal to 1.5°. We can see from the diffraction patterns that the peaks intensity increases as the

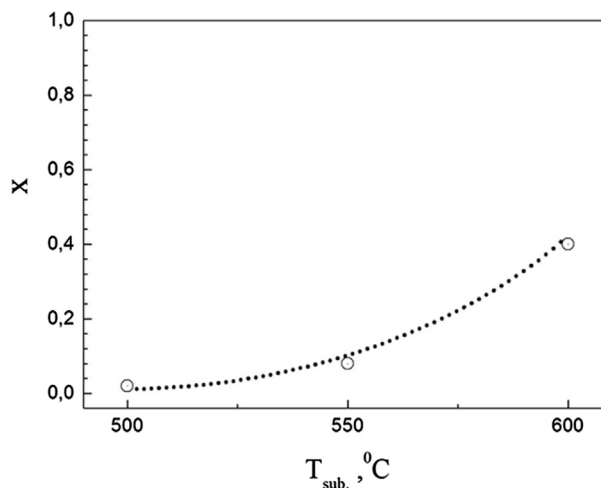


Fig. 2. Dependence of the composition of $\text{Zn}_x\text{Sn}_{1-x}\text{Se}$ films on substrate temperature.

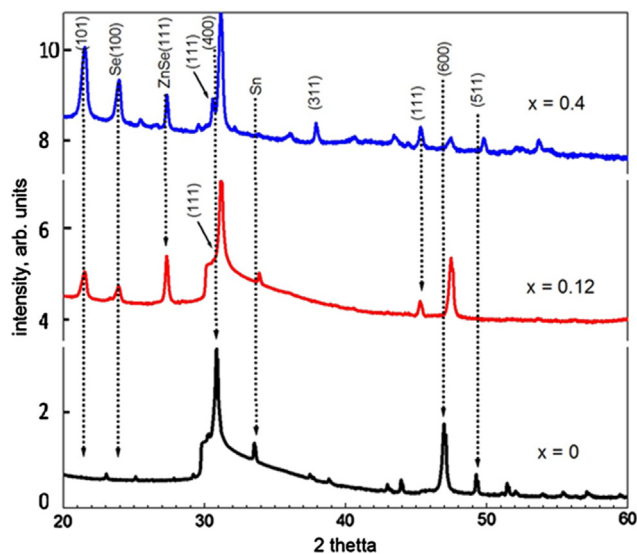


Fig. 3. X-ray diffraction patterns of ZTSe films with different compositions.

composition x increases. Moreover, (4 0 0) peak moves to high theta side with increasing Zn content in ZTSe. The samples had orthorhombic and cubic structures depending on Zn content in ZTSe. The films had orthorhombic structure at composition $x = 0$. We observed the increasing of the cubic structure with content of ZnSe in ZTSe films. XRD has shown that samples have ZnSe, SnSe, Se and Sn phases as well.

SEM pictures (Fig. 4) show the polycrystalline structure of the samples. The crystallite size of films was calculated using Debye-Scherrer’s formula, $D = 0.9\lambda/\beta \cos(\theta)$, where ‘D’ is the average crystallite size, ‘ λ ’ is the wavelength of the incident x-ray beam (0.1514 nm), ‘ β ’ is the full width half maxima value and ‘ θ ’ is diffraction angle (Henry et al., 2017). The average crystallite size of films was calculated to be in the range of (2–20) μm depending on the substrate temperature. The grain size of samples increased from (2–5) μm to (15–20) μm for substrate temperatures of 500 $^{\circ}\text{C}$ and 550 $^{\circ}\text{C}$ respectively. While, at substrate temperature of 600 $^{\circ}\text{C}$ the grain size decreased up to (3–5) μm , possibly, because of increasing of ZnSe content.

Fig. 5 shows the absorption spectra of ZTSe films with different compositions fabricated at substrate temperature of 550 $^{\circ}\text{C}$ in the wavelength range of 300–1500 nm. The precursors had different compositions: SnSe for $x = 0$, Zn/Sn = 0.8 for $x = 0.12$ and Zn/Sn = 1.8 for $x = 0.3$. The band gap of the films was calculated by plotting $(\alpha h\nu)^2$ against $h\nu$. The band-gap values were determined from the intercept of the straight-line portion of the $(\alpha h\nu)^2$ against $h\nu$ graph on the $h\nu$ axis. The band gap increased with ZnSe precursor temperature from 1.0 eV to 2.1 eV. This is due to by the fact that the band gap of ZnSe is high (2.7 eV) than the band gap of SnSe (1.0 eV).

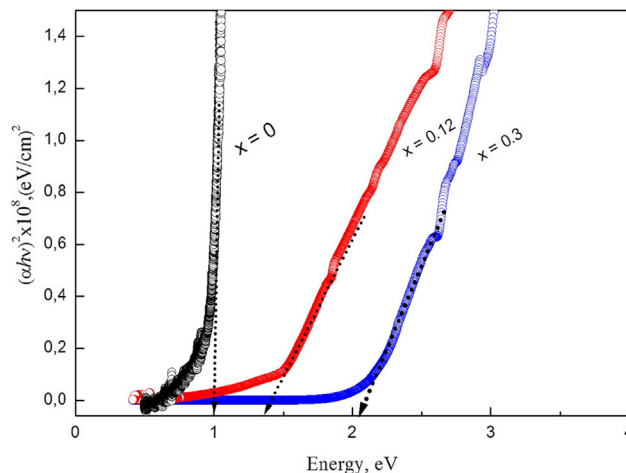


Fig. 5. The absorption spectra of ZTSe films with different compositions fabricated at substrate temperature of 550 $^{\circ}\text{C}$.

Table 1
Electrical parameters of ZTSe films.

Tsub ($^{\circ}\text{C}$)	Composition of films	σ ($\Omega \times \text{cm}$) $^{-1}$	$E_{\text{activation}}$ (eV)	Type of conduct
500	$x = 0.026$	100	0.02	p
550	$x = 0.04$	25	0.04	p
600	$x = 0.4$	1×10^{-6}	0.22	n

Electrical parameters of ZTSe films fabricated at different substrate temperatures are presented in Table 1. It is seen that the conductivity of samples decreases with the substrate temperature. The conductivity of samples fabricated at 500 $^{\circ}\text{C}$ and 550 $^{\circ}\text{C}$ were 100 and 25 ($\Omega \times \text{cm}$) $^{-1}$ respectively. The conductivity of the sample fabricated at the substrate temperature of 600 $^{\circ}\text{C}$ significantly decreased up to 10^{-6} ($\Omega \times \text{cm}$) $^{-1}$. It is caused owing to low conductivity of ZnSe film (10^{-12} ($\Omega \times \text{cm}$) $^{-1}$), since the content of ZnSe increases with the substrate temperature of ZTSe films (Fig. 2). Moreover, we have observed the inversion of the type of conductivity. The samples fabricated at substrate temperatures of 500 $^{\circ}\text{C}$ and 550 $^{\circ}\text{C}$ had p-type of conductivity. While the sample fabricated at a substrate temperature of 600 $^{\circ}\text{C}$ showed n-type conductivity. This is probably due to the fact that ZnSe film has n-type conductivity, therefore ZTSe film with $x \geq 0.4$ performed n-type conductivity.

4. Conclusion

The ZTSe films have been fabricated by chemical molecular beam deposition in atmospheric pressure hydrogen flow at substrate

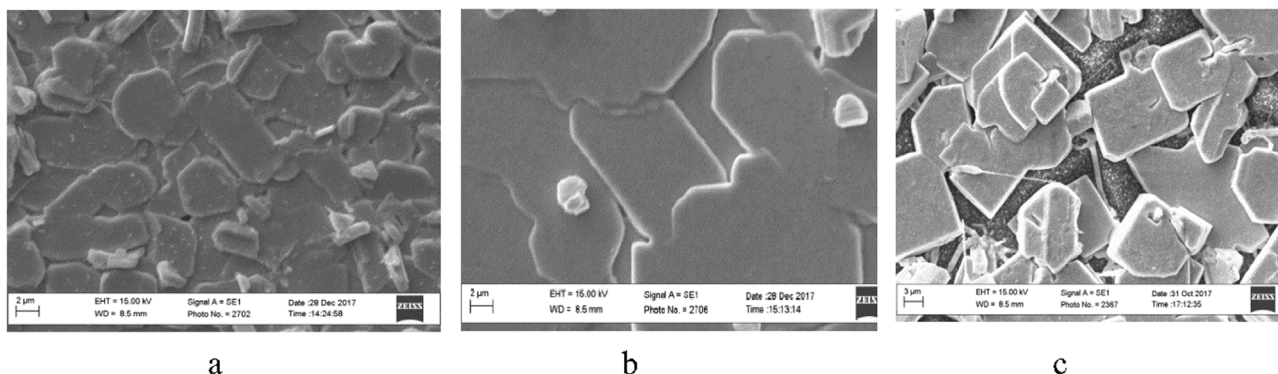


Fig. 4. SEM images of ZTSe films fabricated at different substrate temperatures: (a) $T_s = 500$ $^{\circ}\text{C}$; (b) $T_s = 550$ $^{\circ}\text{C}$; (c) $T_s = 600$ $^{\circ}\text{C}$.

temperatures of 500 °C, 550 °C and 600 °C for the first time. XRD, SEM, optical and electrical properties were studied. The composition of $Zn_xSn_{1-x}Se$ films moves to ZnSe side with the increasing the deposition temperature. The samples had cubic and orthorhombic structure with the grain size of (2–20) μm . The optical band gap increased as the composition of ZTSe moves to ZnSe side. We observed an inversion of the type-conductivity from p- to n-type and the decreasing of the conductivity as x increases.

Acknowledgement

This work was supported by the grant F2-003 of the Basic Research Foundation of the Uzbekistan Academy of Sciences.

References

Green, M.A., Emery, K., Hishikawa, Y., Warta, W., Dunlop, E.D., 2013. Solar cell

- efficiency tables. *Prog. Photovolt: Res. Appl.* 21, 1–11.
- Henry, J., Mohanraj, K., Sivakumar, G., 2017. Effect of pH-induced on the photo-sensitivity of non-toxic Cu_2ZnSnS_4 thin film by chemical bath deposition. *Optik* 311 (141), 139–145.
- Le Donne, A., Trifiletti, V., Binetti, S., 2019. Earth-abundant thin film solar cells based on chalcogenides. *Front. Chem.* 1–14.
- Razykov, T.M., 1991. Chemical molecular beam deposition of II-VI binary and ternary compound films in gas flow. *Appl. Surf. Sci.* 48 (49), 89–92.
- Razykov, T.M., Boltaev, G.S., Bosio, A., Ergashev, B., Kouchkarov, K.M., Mamarasulov, N.K., Mavlonov, A.A., Romeo, A., Romeo, N., Tursunkulov, O.M., Yuldoshov, R., 2018. Characterisation of SnSe thin films fabricated by chemical molecular beam deposition for use in thin film solar cells. *Sol. Energy* 159, 834–840.
- Todorov, T.K., Tang, J., Bag, S., Gunawan, O., Gokmen, T., Zhu, Y., Mitzi, D.B., 2013. Beyond 11% efficiency: characteristics of state-of-the-art $Cu_2ZnSn(S, Se)_4$ solar cells. *Adv. Energy Mater.* 3, 34–38.
- Wang, W., Winkler, M.T., Gunawan, O., Gokmen, T., Todorov, T.K., Zhu, Y., Mitzi, D.B., 2014. Device characteristics of CZTSSe thin-film solar cells with 12.6% efficiency. *Adv. Energy Mater.* 4 (7), 1301465.